Science of the Total Environment 654 (2019) 1293–1304

Contents lists available at ScienceDirect

Science of the Total Environment

journal homepage: www.elsevier.com/locate/scitotenv

Using Pb isotope ratios of particulate matter and epiphytic lichens from the Athabasca Oil Sands Region in Alberta, Canada to quantify local, regional, and global Pb source contributions

Joseph R. Graney [a,*], Eric S. Edgerton [b], Matthew S. Landis [c]

[a] Geological Sciences and Environmental Studies, Binghamton University, Binghamton, NY, USA
[b] Atmospheric Research & Analysis, Inc., Cary, NC, USA
[c] Integrated Atmospheric Solutions, LLC., Cary, NC, USA

HIGHLIGHTS

- Pb isotopes measured in $PM_{2.5}$ and $PM_{10-2.5}$ from Fort McKay, Alberta in 2010–2011
- Eastern Asia sources contributed 47% of the Pb in the $PM_{2.5}$ in 2010–2011.
- Pb isotopes measured in lichens around mining operations in 2008, 2011, and 2014
- 46% of the lichen Pb from regional, 32% from local, and 22% from global sources

GRAPHICAL ABSTRACT

Air Monitoring Site in Ft. McKay, Alberta used for Pb Source Attribution Study

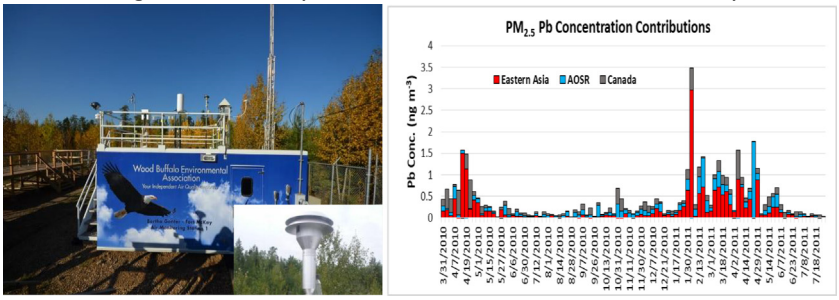

Inset is enlargement of dichotomous sampler inlet used to collect Particulate Matter (PM)

ARTICLE INFO

Article history:
Received 5 July 2018
Received in revised form 3 November 2018
Accepted 4 November 2018
Available online 6 November 2018

Guest Editor: Kelly Roland Munkittrick

Keywords:
Pb isotopes
Particulate matter
Fugitive dust
Eastern Asian Pb sources
Global transport of aerosols

ABSTRACT

Ambient air particulate matter (PM) was collected at the Wood Buffalo Environmental Association Bertha Ganter Fort McKay monitoring station in the Athabasca Oil Sand Region (AOSR) in Alberta, Canada from February 2010 to July 2011 as part of an air quality source assessment study. Daily 24-hour duration fine ($PM_{2.5}$) and coarse ($PM_{10-2.5}$) PM was collected using a sequential dichotomous sampler. 100 pairs of $PM_{2.5}$ and $PM_{10-2.5}$ were selected for lead (Pb) concentration and isotope analysis. Pb isotope and concentration results from 250 epiphytic lichen samples collected as far as 160 km from surface mining operations in 2008, 2011, and 2014 were analyzed to examine longer term spatial variations in Pb source contributions. A key finding was recognition of thorogenic ^{208}Pb from eastern Asia in the springtime in the $PM_{2.5}$ in 2010 and 2011. $^{206}Pb/^{207}Pb$ and $^{208}Pb/^{207}Pb$ isotope ratios were used in a three-component mixing model to quantify local, regional, and global Pb sources in the PM and lichen data sets. 47 ± 3% of the Pb in the $PM_{2.5}$ at AMS-1 was attributed to sources from eastern Asia. Combined results from $PM_{10-2.5}$ and $PM_{2.5}$ indicate $PM_{2.5}$ Pb contributions from eastern Asia (34%) exceed local AOSR sources of $PM_{2.5}$ Pb (20%), western Canada sources of $PM_{2.5}$ Pb (19%), and $PM_{10-2.5}$ Pb from fugitive dust including oil sands (14%), tailings (10%), and haul roads (3%). The lichen analysis indicates regional sources contribute 46% of the Pb, local sources 32%, and global sources 22% over the 2008–2014 timeframe. Local sources dominate atmospheric Pb deposition to lichens at near field sites (0–30 km from mining operations) whereas regional Pb sources are prevalent at distal sites (30–160 km). The Pb isotope methodology successfully quantified trans-

* Corresponding author.
E-mail address: jgraney@binghamton.edu (J.R. Graney).

https://doi.org/10.1016/j.scitotenv.2018.11.047

Pacific transport of Pb to the AOSR superimposed over the aerosol footprint of the world's largest concentration of bitumen mining and upgrading facilities.

1. Introduction

The Athabasca Oil Sands Region (AOSR) in northeastern Alberta, Canada contains the world's largest concentration of bitumen production and upgrading facilities with economically recoverable petroleum reserves estimated to be approximately 165 billion barrels in 2016 (Alberta Energy Regulator, 2018). Oil production from surface mining operations in the AOSR began in 1967 and has increased from 0.38 million barrels per day in 2000, to 1.24 million barrels per day in 2016 (Alberta Energy Regulator, 2018). Quantifying ambient particulate matter (PM) concentrations and atmospheric deposition from this large scale industrial activity is essential to inform emission mitigation strategies in the AOSR and to address human and ecosystem health concerns. Landis et al. (2017) quantified ambient fine ($PM_{2.5}$) and coarse ($PM_{10-2.5}$) concentrations and sources from aerosols collected in 2010–2011 within the Fort McKay First Nation and Metis community in the AOSR using the U.S. Environmental Protection Agency implemented positive matrix factorization (PMF) receptor model. Fort McKay is located centrally within the footprint of the AOSR surface mining operations (Fig. 1). A $PM_{2.5}$ lead (Pb) factor was identified by PMF that had a pronounced seasonality component with enhanced contributions during the spring of 2010 and the spring of 2011. This seasonal pattern did not appear to be correlated with known emissions from local or regional sources, but is consistent with previously observed trans-Pacific transport of pollution from Asia to western North America (Yienger et al., 2000; VanCuren and Cahill, 2002; VanCuren, 2003).

Pb can be emitted into the atmosphere by high temperature anthropogenic processes including non-ferrous metal smelting, battery recycling, coal combustion, waste incineration, and aviation fuels (U.S. EPA, 2015). Once emitted, lead may be transported on local, regional, or intercontinental scales depending on several factors, including particle size, the elevation of emission, and meteorology. Based on multi-element studies, long range transport to the North Pacific region and adjacent land masses in western North America can include large contributions of Pb from eastern Asian sources superimposed over local sources (Uematsu et al., 1983; Jaffe et al., 1999; Zdanowicz et al., 2006; Osterberg et al., 2008) with the contributions from eastern Asian sources enhanced in the springtime (Fischer et al., 2009).

We hypothesized that Pb isotope analysis could be used to quantify contributions from Pb sources on local, regional, and global scales in the AOSR. Pb has four major isotopes, 204, 206, 207, and 208. ^{208}Pb is formed from the radioactive decay of ^{232}Th, ^{207}Pb from ^{235}U, and ^{206}Pb from ^{238}U. ^{204}Pb is referred to as common Pb (has no radioactive parent, and is much less abundant than the other isotopes). The uranium and thorium parents have differing decay rates resulting in predictable changes in Pb isotope ratios (Faure, 1986). The Pb isotope ratios from PM sources can reflect the age at which Pb was incorporated into parent material (e.g., ore deposit, coal, oil) and are preserved without fractionation during the subsequent process that emitted the Pb into the

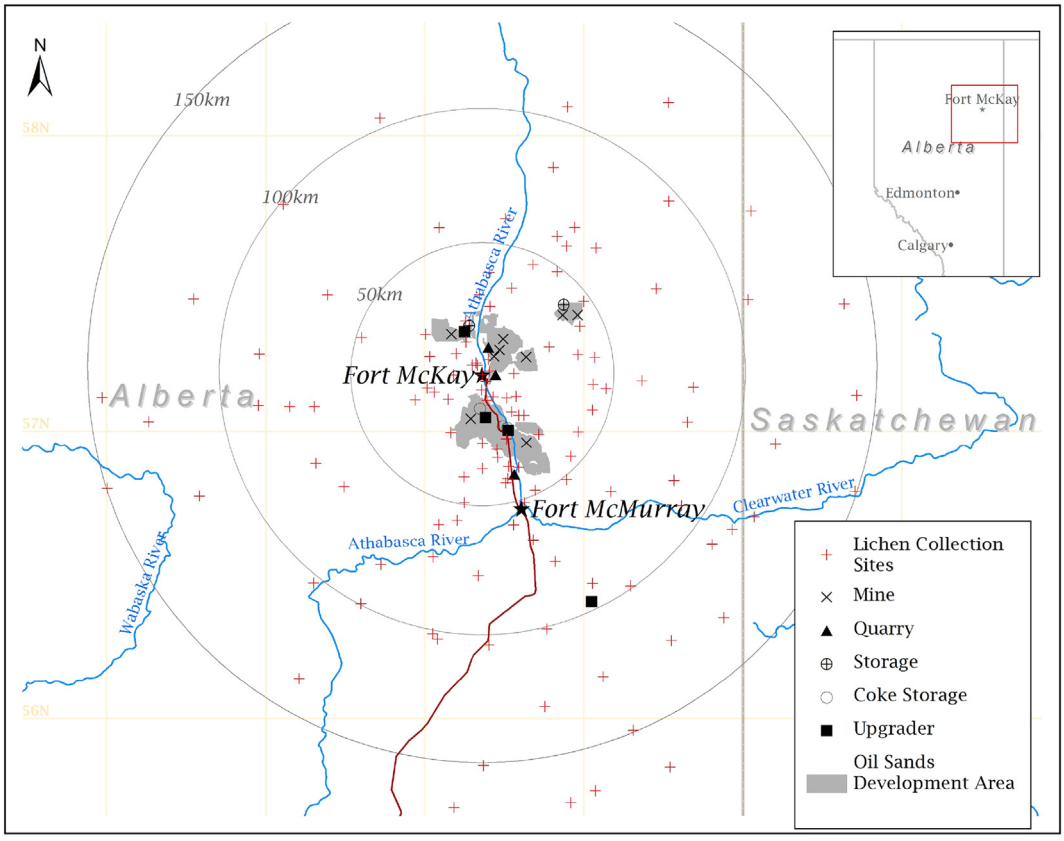

Fig. 1. WBEA Fort McKay ambient monitoring station (star symbol) in relation to lichen collection sites and major surface oil sand mining and production facilities in northeastern Alberta, Canada (inset).

environment (Graney et al., 1995). Following emission from high temperature processes, Pb species quickly nucleate or condense onto atmospheric aerosols. The use of Pb isotopes to help determine the sources and sinks of Pb emitted to the atmosphere has been summarized in Komarek et al. (2008). In relation to the objectives of this study, Pb isotopes have been used to document regional and local emission, transport, and deposition processes using epiphytic lichens in Europe (Cloquet et al., 2006), eastern and western Canada (Carignan and Gariepy, 1995; Carignan et al., 2002; Simonetti et al., 2003) and the AOSR (Graney et al., 2012). Such an approach using PM has not been attempted in the AOSR.

Recent PM studies concluded that after the phasing out of the use of leaded gasoline in China (Zheng et al., 2004; Chen et al., 2005; Wang et al., 2006), energy generation processes, predominantly coal combustion, are the major source of Pb emissions to the atmosphere in eastern Asia with smaller contributions from metal refining (Chen et al., 2008; Kong et al., 2011; Li et al., 2012). The atmospheric emissions from China are characterized by lead from thorogenic sources (Mukai et al., 1993; Bellis et al., 2005; Cheng and Hu, 2010) which results in higher $^{208}Pb/^{207}Pb$ and $^{208}Pb/^{206}Pb$ than lead from other sources (Bollhöfer and Rosman, 2001; Tan et al., 2006). Thorogenic Pb has been used to identify contributions from eastern Asia to lake sediment in Japan (Hosono et al., 2016), the North Pacific Ocean (Gallon et al., 2011), PM in the western United States (Ewing et al., 2010) as well as ice cores in western Canada (Gross et al., 2012) and Greenland (Bory et al., 2014; Kang et al., 2017). However, a thorogenic ^{208}Pb component representing long distance transport to and deposition within the AOSR has yet to be documented.

Based on the results from metal accumulation in peat cores in the AOSR, Shotyk et al. (2017) recommended that particle size and transport distance need to be better constrained in source assessments in the AOSR. Lichens (as well as peat cores) integrate deposition over long time scales (years), so to better determine what proportion of the Pb in the PM in the AOSR is from Asian sources rather than regional or local sources shorter sampling intervals, such as daily sampling, may be needed. Previous work on lichens collected in the AOSR (Graney et al., 2012) had indicated differences in Pb isotope ratios and elemental concentrations related to the distance from mining and processing operations that may have been related to PM size and transport regimes. So, this study combines Pb concentration and isotope measurements from $PM_{2.5}$ and $PM_{10-2.5}$ data sets to distinguish between aerosol sources. One goal of this study was determining whether a thorogenic eastern Asia ^{208}Pb signature could be recognized and quantified in PM collected within the large industrial PM fingerprint associated with oil sands mining and processing from a remote region within the boreal forest in western Canada. We will demonstrate that the use of Pb isotope ratios from 24-h duration PM samples coupled with findings from lichens can provide both short-term temporal and long-term spatial resolution for quantifying Pb in the AOSR from local, regional, and global PM sources.

2. Methods

2.1. Particulate matter sampling site

The Wood Buffalo Environmental Association (WBEA) Bertha Ganter-Fort McKay (BGFM) ambient air monitoring station (57°11′ 21.70″ N; −111°38′26.06″ W) is located in the Fort McKay First Nation and Metis community. The BGFM site is located in an area that is in close proximity to ongoing oil sand production operations such as surface mining, hauling, separating, and upgrading of bitumen (Fig. 1). Twenty-four-hour ambient PM samples for mass and element determinations were collected on a daily basis from February 22, 2010 through July 27, 2011 using a ThermoScientific Model 2025D Sequential Dichotomous air sampler (a U.S. Environmental Protection Agency (EPA) designated Federal Equivalent Method for $PM_{2.5}$). The dichotomous sampler had a PM_{10} impactor inlet operating at 16.7 LPM to make the initial particle size cutoff at 10 μm mass median aerodynamic diameter (MMAD). The virtual impactor in line after the PM_{10} impactor inlet acts as a dichotomous splitter and dynamically segregates the particles into fine (≤2.5 μm) and coarse (10–2.5 μm) size fractions (Loo and Cork, 1998). The $PM_{2.5}$ and $PM_{10-2.5}$ size fractions were collected onto two separate 47 mm Teflon membrane filters (Measurement Technologies Laboratories, Minneapolis, MN) with Teflon support rings. Calibrated mass flow controllers maintained the fine particle filter flow at 15.0 LPM and the coarse particle filter flow at 1.67 LPM to ensure the correct MMAD size cut.

The use of a virtual impactor results in the collection of all coarse mode particles from the total flow and the fine mode particles in the minor flow on the coarse filter (McFarland et al., 1978). The coarse mode results (mass and element concentrations as well as Pb isotopes) are adjusted for the fine mode contribution as discussed in Landis et al. (2017). Details on the pre- and post-sampling filter weighing, sample collection, and shipment protocols performed by Atmospheric Research & Analysis, Inc., (ARA; Cary, North Carolina, USA) are presented in Landis et al. (2017).

2.2. Filter selection for element and Pb isotope analysis

Over the course of the study, 392 valid daily dichotomous $PM_{2.5}$ and $PM_{10-2.5}$ sample pairs were collected with mean concentrations of 6.8 ± 12.9 μg m^{-3} (mean ± standard deviation) and 6.9 ± 5.9 μg m^{-3}, respectively. A subset of 100 dichotomous sample pairs was selected for elemental concentration and Pb isotope analysis. The selected samples included an even distribution across the seasons. Landis et al. (2017) provides further details on the sample selection criteria.

2.3. Lichen collection for Pb isotope analysis

Lichen samples for Pb isotope analysis were collected within an approximate 160 km radius from the center of AOSR surface oil sand production operations (Fig. 1) using a scaled (nested) approach in 2008 (n = 121 sites) and 2014 (n = 127 sites). (Edgerton et al., 2012; Landis et al., 2018). A higher density of sites was located closer to the major mining and processing operations with a decreasing frequency as the distance from the oil sands production areas increased. A smaller number of samples were collected in summer 2011 (n = 21 sites) overlapping the time frame when the PM samples were obtained. Bulk composite samples of the epiphytic lichen *Hypogymnia physodes* were collected from branches from a minimum of 10 standing jack pine (*Pinus banksiana*) or black spruce (*Picea mariana*) trees at approximately 1.5 m off the ground at each sampling site. Several grams of lichen were collected at each site and specimens from all the trees were composited into the same, pre-cleaned 500 ml amber glass jar (Fisher Scientific; #02-993-053), Lichen samples were cleaned by removing all foreign materials (bark and other debris), then dried, and ground to a fine powder using a zirconium ball mill (Edgerton et al., 2012).

2.4. Sample extraction and analysis

The PM and lichen samples were digested using a CEM Corporation (Matthews, NC) Mars Express microwave digestion system in a mixture of ultra-pure H_2O_2, HF and HNO_3 in a procedure similar to that developed by Jalkanen and Häsänen (1996). The sample extracts from the PM and lichens samples were then analyzed for a suite of elements using a Perkin-Elmer (Waltham, MA) Model 9000 Elan-II dynamic reaction cell inductively coupled plasma mass spectrometer (DRC-ICPMS). Further details of the procedures are provided in Edgerton et al. (2012) and Landis et al. (2017) and are summarized in the Appendix.

2.5. Pb isotope ratio analysis

The remaining sample (typically 10 ml) from the filter and lichen digests that had been used for the multi-element determinations were subsequently measured for stable Pb isotopes using a Thermo Scientific (Franklin, Massachusetts, USA) model Element2 inductively coupled plasma high resolution magnetic sector field mass spectrometer (ICP-SFMS). The method used to measure the Pb isotope ratios has been described in detail in Graney et al. (2012), and included: (i) self-aspiration of sample through a cyclonic spray chamber with an uptake rate of 200 μl min^{-1} to maximize signal stability; (ii) optimization of the detector dead time in the scanning speed operation mode; (iii) utilization of low resolution detection mode to produce flat-topped peak shapes; (iv) use of a narrow mass width window (10% of the peak top-width) scanned at a high sweep rate, and (v) as needed, sample concentrations were diluted to less than 2 ppb Pb concentrations to optimize isotope ratio acquisition. A bracketing technique was used to correct for potential mass bias during measurement of the Pb isotope ratios using NIST SRM 981 (Krachler et al., 2004; Yip et al., 2008). In this study, the Pb isotope ratios from the NIST SRM 981 were measured before and after four replicate analyses of each of the PM or lichen samples to correct the results for ICP-SFMS mass bias (Krachler et al., 2004; Graney et al., 2012).

3. Results and discussion

3.1. Fort McKay ambient dichotomous sample element results

The subset of 100 dichotomous sample pairs selected for element and Pb isotope analysis had an average $PM_{2.5}$ mass concentration of 8.6 ± 21.6 μg m^{-3} and $PM_{10-2.5}$ of 7.6 ± 5.8 μg m^{-3} with the temporal variability presented in Fig. 2a–b. Wildland fires made a major contribution to the $PM_{2.5}$ mass in late May of 2011. The overall concentration of Pb was greater in the $PM_{2.5}$ (0.393 ± 0.498 ng m^{-3}) than $PM_{10-2.5}$ (0.136 ± 0.122 ng m^{-3}), and Pb concentration in the $PM_{2.5}$ was consistently higher than $PM_{10-2.5}$ in April – May 2010 and January–May 2011 (Fig. 2c–d). In contrast, the S and Al concentrations showed more variability on a day-to-day basis (SI Figs. A.1), with S concentrations typically higher in the $PM_{2.5}$ (378.8 ± 251.8 ng m^{-3}), than the $PM_{10-2.5}$ (44.85 ± 34.73 ng m^{-3}), and the Al concentrations typically higher in the $PM_{10-2.5}$ (300.5 ± 261.7 ng m^{-3}), than the $PM_{2.5}$ (41.39 ± 38.06 ng m^{-3}). These results suggest that the source(s) of the Pb are partially decoupled from the PM, S, and Al sources. The springtime enhancements in the concentrations of Pb in the $PM_{2.5}$ suggest an important seasonal source signal that is superimposed over those from oil sands mining and processing which operates year-round.

Application of the U.S EPA implemented PMF receptor model on the 100 Fort McKay ambient PM samples used for this Pb isotope study resolved six $PM_{10-2.5}$ sources which explained 99% of the mass (Landis et al., 2017) including fugitive dust from haul roads, oil sands mining, mixed anthropogenic sources, biomass combustion, and mobile sources which includes emissions from the mining fleet (SI Fig. A.2a). PMF resolved five $PM_{2.5}$ sources which explained 96% of the mass including oil sands upgrading, biomass combustion, mixed source fine fugitive dust, a Pb source, and road salt. (SI Fig. A.2b). The Pb source accounted for 9% of the $PM_{2.5}$ mass.

Prior PM and lichen biomonitoring studies have identified the fugitive emission of $PM_{10-2.5}$ from oil sand production activities as the primary driver of the observed near field atmospheric deposition and spatial patterns in the AOSR (Landis et al., 2012; Landis et al., 2017). The temporal variation in the source contributions in the $PM_{2.5}$ and $PM_{10-2.5}$ based on the PMF results are presented in SI Fig. A.2. The $PM_{2.5}$ Pb source factor identified in the PMF source apportionment demonstrates a seasonal temporal trend (SI Fig. A.2b) corresponding with two primary episodes of enhanced Pb concentrations observed during the spring of 2010 and the spring of 2011 (Fig. 2c). Other elements with significant loading on this factor were As, Zn, and Cd (Landis

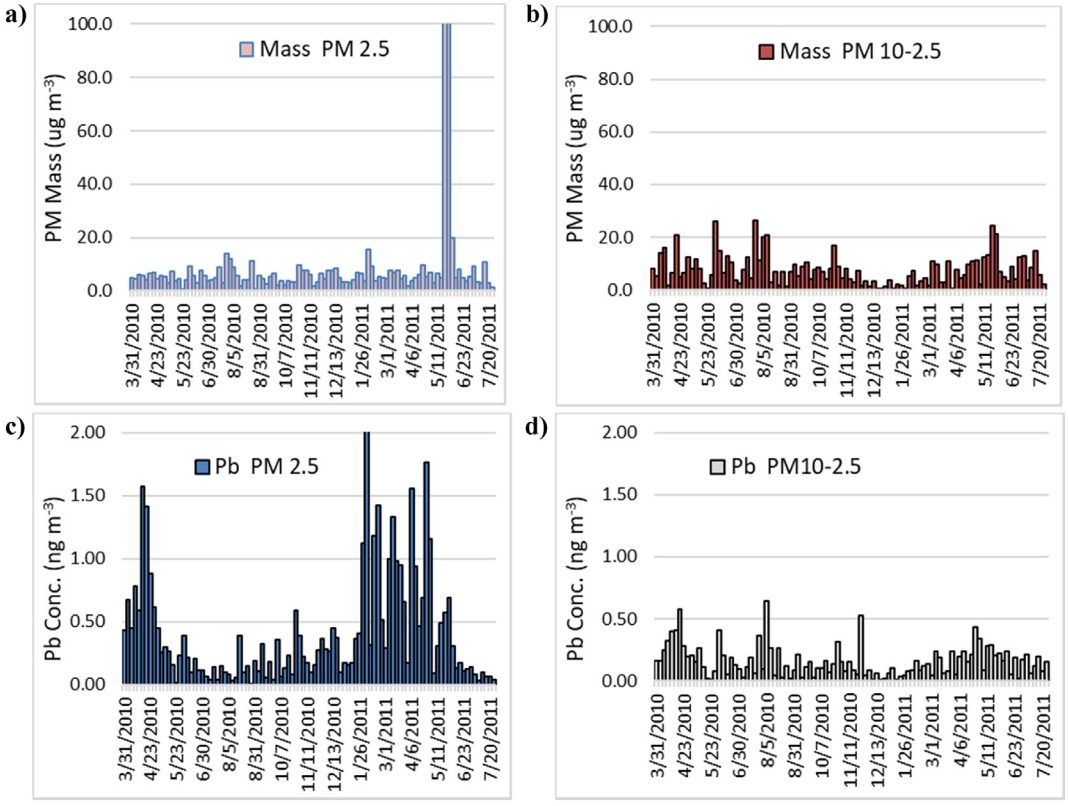

Fig. 2. Temporal results from the $PM_{2.5}$ and $PM_{10-2.5}$ samples collected in Ft. McKay in 2010 and 2011 for a) $PM_{2.5}$ mass, b) $PM_{10-2.5}$ mass, c) $PM_{2.5}$ lead (Pb), and d) $PM_{10-2.5}$ lead (Pb) concentrations.

et al., 2017). This multi-element signature could reflect high temperature anthropogenic emission processes such as coal combustion or smelter emissions associated with long distance transport.

PM studies indicate that the Pb concentration in aerosols collected in eastern Asia can be as much as a factor of 100 greater than those measured in Ft. McKay. Pb concentrations as high as several hundred ng m^{-3} have recently been reported in several locations in China (Schleicher et al., 2011; Widory et al., 2010; Wang et al., 2015a, 2015b; Zhou et al., 2016) versus the several ng m^{-3} typical in Ft. McKay (this study, Fig. 2c). Because the Ft. McKay aerosol Pb concentrations are relatively low compared to sampling sites from eastern Asia, it may be feasible to determine if Pb from eastern Asia is transported to the AOSR in trans-Pacific aerosol plume events prevalent in the spring (Fischer et al., 2009; Gross et al., 2012). The signature of these events would be superimposed over local and regional Pb sources that might be decoupled by using Pb isotope ratio analysis.

3.2. Fort McKay ambient dichotomous sample Pb isotope results

The $^{206}Pb/^{207}Pb$ and $^{208}Pb/^{207}Pb$ isotope ratios from the $PM_{10-2.5}$ and $PM_{2.5}$ samples from Ft. McKay are plotted in Fig. 3a. A visual interpretation of the $PM_{10-2.5}$ data within Fig. 3a results in an elliptical field that in general has higher $^{206}Pb/^{207}Pb$ and $^{208}Pb/^{207}Pb$ than the field that encompasses the $PM_{2.5}$ samples. When the $PM_{10-2.5}$ and $PM_{2.5}$ results from the same sample collection day are examined, the $PM_{10-2.5}$ samples almost always have higher $^{206}Pb/^{207}Pb$ and $^{208}Pb/^{207}Pb$ than the corresponding $PM_{2.5}$ samples (Fig. A.3 in Appendix). Because the PM sources that contribute to the $PM_{10-2.5}$ and $PM_{2.5}$ differ based on the PMF source apportionment results, it is possible Pb isotopes might also impart a signature that reflects differences in PM sources. That possibility is explored in the next section.

3.3. Results and insights from Pb isotopes from source and soil samples from the AOSR

Pb isotopes were measured on source samples from the AOSR including exposed (weathered) and fresh oil sands, processed materials produced during the upgrading operations (including petroleum coke) as well as upgrader stack emissions, and the sand and clay from tailings ponds, limestone from quarrying operations used to construct haul roads, and PM from heavy hauler fleets (Fig. 3b). Details concerning the collection and composition of source samples are provided in Landis et al., 2012, 2017. The PM source samples from upgrader stacks and the heavy hauler fleet were collected using dilution systems to allow aerosols to form via condensation and coagulation as the exhaust stream cools to ambient temperature (Wang et al., 2012; Watson et al., 2012; Wang et al., 2016). In addition, soils from lichen sample sites were collected and analyzed for Pb isotopes in a prior study (Graney et al., 2017) and are included in Fig. 3b. The processed material and stack samples had the highest $^{208}Pb/^{207}Pb$ and $^{206}Pb/^{207}Pb$ ratios whereas the fleet, tailings and soils had lower $^{208}Pb/^{207}Pb$ and $^{206}Pb/^{207}Pb$ ratios, with the weathered and fresh oil sands displaying a wide range of Pb isotope ratios. The Pb isotopes from the fresh and weathered oil sands samples plot within an elliptical field that does not intersect the processed material and stack samples (Fig. 3b).

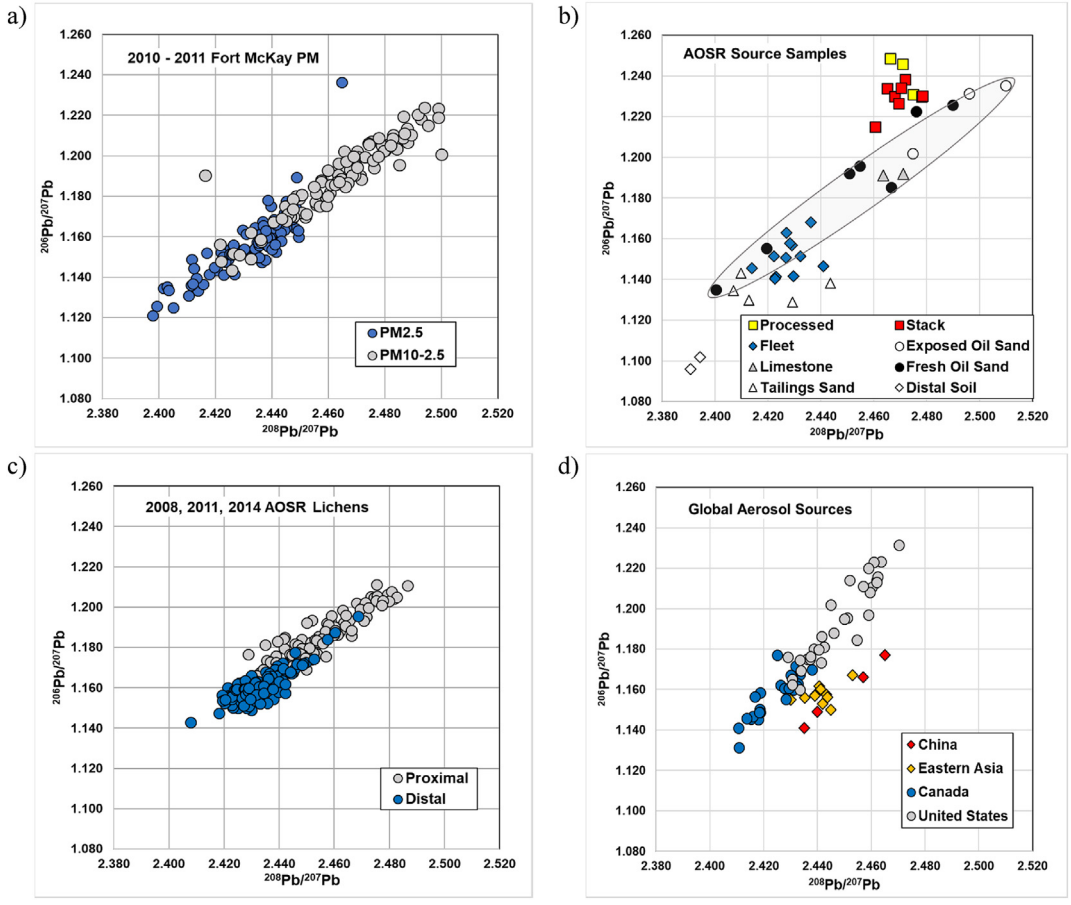

Fig. 3. Pb isotope results from a) Fort McKay ambient 2010–2011 PM samples, b) source samples from the AOSR, c) lichens collected in 2008, 2011, and 2014 at sites proximal (< 30 km) and distal (30–160 km) from surface oil sands mining operations, and d) aerosols from cities in China, Eastern Asia, Canada, and the United States (compiled from Bollhöfer and Rosman, 2001, 2002 datasets). The average 2σ error of the Pb isotope ratios for the PM and lichen samples is the same size as the diameter of the data points for $^{206}Pb/^{207}Pb$ (y-axis) and twice the size of the diameter of the data points for $^{208}Pb/^{207}Pb$ (x-axis). The elliptical field in Fig. 3b encompasses the results from the fresh and exposed (weathered) oil sands samples.

In the AOSR near field (<30 km from major surface mining operations) atmospheric pollution mainly consists of fugitive $PM_{10-2.5}$ emissions (wind-blown dust) and $PM_{2.5}$ diesel engine combustion exhaust from shovel and truck fleet operations and stack emissions (Landis et al., 2012; Wang et al., 2015b). Therefore, the ambient $PM_{2.5}$ near mining operations likely contains a large component of combustion exhaust, whereas the $PM_{10-2.5}$ contributions are likely a mixture from several fugitive dust sources. The PM from the fleet samples, as well as the PM from other high temperature combustion processes such as oil sands upgrading, should be $PM_{2.5}$ dominant whereas the oil sand, limestone, and tailing sands would be predominantly in the $PM_{10-2.5}$ fraction (Landis et al., 2017). The Pb isotope ratios from the ambient Fort McKay samples likely reflect this expectation, with $PM_{2.5}$ ratios most similar to values from the fleet samples, and $PM_{10-2.5}$ ratios consistent with a mixture of the oil sand, limestone, and tailing sands values (Figs. 3a–b). The Fort McKay ambient PM sample results do not suggest a major PM contribution from bitumen upgrading stack emissions based on the extent of the fields for either the $PM_{10-2.5}$ or $PM_{2.5}$ Pb isotope results. It is possible that the stack emissions would be reflected more regionally due to plume dispersion and atmospheric deposition dynamics rather than contributing to significant near field deposition. Because the BGFM site in Fort McKay is located in close proximity to several of the surface mining and upgrading facilities, ambient PM at this site was expected to be heavily impacted by nearfield fugitive dust sources (Landis et al., 2012). To assess more regionally representative atmospheric Pb deposition information, sampling sites further from mining and upgrading operations are needed. Lichen samples were collected and analyzed to provide this spatial resolution.

3.4. Results and insights from Pb isotopes from lichen samples from the AOSR

Lichen samples were collected in the AOSR in 2008 (121 sites), 2011 (21 sites) and 2014 (128 sites) to assess element and Pb isotope spatial atmospheric deposition patterns proximal (near field, <30 km) and distal (30–160 km) from mining operations (Edgerton et al., 2012; Graney et al., 2012, Landis et al., 2017). Based on previous work in the AOSR, it has been demonstrated that the Pb isotope composition of lichens is a better indicator of source strength than Pb concentrations (Graney et al., 2012). The Pb isotope results from the lichens collected from 2008 to 2014 suggest a decrease in $^{206}Pb/^{207}Pb$ and $^{208}Pb/^{207}Pb$ from the near field to distal sites (Fig. 3c) suggesting a larger influence of $PM_{10-2.5}$ at the near field sites, and a greater contribution of $PM_{2.5}$ at the distal sites. The clustering of the results into the two groupings is similar to the results from the ambient Fort McKay PM samples. The lichen results plot in elliptical fields that have a smaller magnitude in Pb isotope space than the Fort McKay ambient PM results likely due to homogenization of the $PM_{2.5}$ and $PM_{10-2.5}$ isotope signatures during accumulation by the lichens.

3.5. Insights from Pb isotopes from aerosol samples from other studies

Pb isotope measurements from aerosols from other regional and global scale studies provide insights to document long range transport superimposed over local source contributions in the AOSR. The Pb isotope results from aerosols collected in urban areas by Bollhöfer and Rosman (2001 and 2002) are presented in Fig. 3d. Samples from cities in China, other cities in Eastern Asia, Canada, and the United States (US) are included in this plot. Note that the US and Canada aerosols overlap in isotope space, with the US aerosols typically having higher $^{206}Pb/^{207}Pb$ and $^{208}Pb/^{207}Pb$ than the samples from Canada. Interestingly, the samples from the cities in the US with the highest $^{206}Pb/^{207}Pb$ and $^{208}Pb/^{207}Pb$ are from coastal areas where oil-fired power plants are located (e.g., Tampa Florida; Pancras et al., 2011). The samples from these coastal cities lie along a linear isotope space array that would intersect the source signature for samples from the stack and process samples from the AOSR. The AOSR samples likely represent the Pb isotope signature for synthetic crude oil upgraded from bitumen, and may be representative of the Pb isotope signature emitted by other oil combustion facilities as well. Note that the samples from China plot along a linear trend that is offset from the US and Canada field. Specifically, the samples from China are offset in Pb isotope space along a trend that has a higher $^{208}Pb/^{207}Pb$ at similar $^{206}Pb/^{207}Pb$ values. This reflects a greater thorogenic ^{208}Pb component in the China samples in comparison to the US and Canada samples that has been noted in several previous studies (Mukai et al., 1993; Bellis et al., 2005; Cheng and Hu, 2010). This Pb isotopic distinction has recently been used to quantify the contribution from eastern Asia in aerosol samples collected in California (Ewing et al., 2010) as well as in ice from western Canada (Gross et al., 2012) and Greenland (Bory et al., 2014; Kang et al., 2017). Visual interpretation of the results from the ambient $PM_{2.5}$ filter samples and distal lichens from the AOSR suggests there may also be a contribution from combustion sources from eastern Asia in these samples. The next section will attempt to quantify this contribution through linking of Pb isotope ratios with Pb concentrations in aerosols from at Fort McKay.

3.6. Quantifying Pb source contributions in $PM_{2.5}$ aerosol samples using Pb isotope ratios

The $^{208}Pb/^{207}Pb$ versus $^{206}Pb/^{207}Pb$ plot for the ambient Fort McKay $PM_{2.5}$ results in a triangular area that encompasses most of the isotope ratio measurements (Fig. 4). The apices of the triangle can be used to estimate the endmember Pb isotope sources that produce the observed isotope ratios by comparison to the results from Fig. 3. The three apices include one isotope composition similar to fleet emissions mixed with stack emissions and fine fugitive oil sands dust from the AOSR (local source endmember), another endmember with an isotopic composition similar to aerosols collected from cities in Canada (regional source), and a third endmember similar to aerosols from eastern Asia (global source). If we assume that these three endmembers comprise the main sources of Pb in the aerosols collected in the AOSR, a three-component mixing model can be used to determine the fractional contribution from the three sources on a sample by sample basis. The measurement of three isotopes of Pb (for example the ^{208}Pb, ^{207}Pb, and ^{206}Pb measured in this study) allows as many as three sources of Pb to be quantified (Gobeil et al., 1995). Pb isotope ratios using measurements from three isotopes of Pb have been used previously to constrain Pb

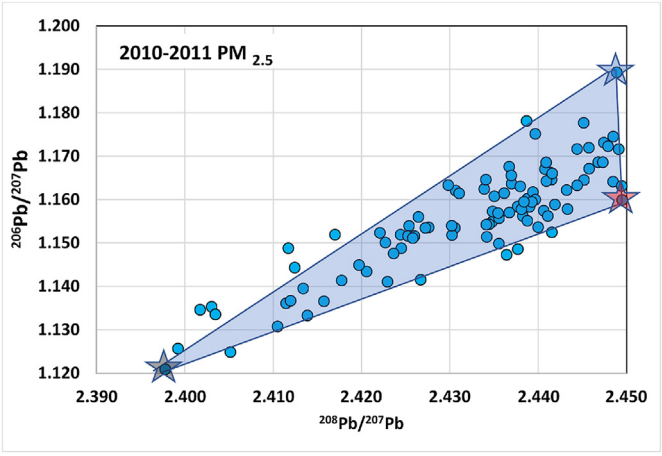

Fig. 4. Fort McKay ambient $PM_{2.5}$ Pb isotope results with proposed endmember compositions from local (AOSR, blue star, upper right), regional (western Canada, gray star, lower left), and global (cities in China, red star, middle right) sources. The triangle encloses the Pb isotope ratios from the samples within the three-endmember spatial field, using sample results to define the apices of the triangle.

sources in sediments (Gobeil et al., 1995) and precipitation samples (Graney and Landis, 2013). The equations for the mixing model and the input parameters for the endmember isotopic compositions used in this study are found in Appendix Table A.1. The input parameters for the eastern Asia source apex of the triangle are the average value of the isotope ratios from the 4 cities in China (Fig. 3d) reported in Bollhöfer and Rosman (2001). The input parameters for the Canadian source apex of the triangle correspond to the values of the lower end of the range in isotope ratios from cities in Canada (Fig. 3d) reported in Bollhöfer and Rosman (2001, 2002). This regional signature could include major contributions from the use of Canadian Pb—Zn ores in aviation fuel and industrial processes near and within urban areas in western Canada as well as smaller contributions from coal-fired power plants in Alberta and smelter emissions from Trail, British Columbia (Environment Canada, 2015). The input parameter for the local AOSR sources corresponds to the values for the third apex of the triangular field. By averaging the Pb isotope results from the fleet emissions and stack emissions (Fig. 3b) and use of a linear mixing calculation, the local AOSR apex of the triangular field corresponds to a mixture of 52% fleet emissions and 48% stack emissions. These are likely maximum estimates for the contributions from fleet and stack emissions to local $PM_{2.5}$, because fugitive dust sources also likely contribute. The results from this three-component source attribution are presented on a temporal basis in Figs. 5a–b and summarized in Table 1.

Note that the contributions from eastern Asia are most pronounced (in many cases over 50%) in April and May of 2010, and in January–May in 2011. This temporal relation matches the time of year in multi-element studies when trans-Pacific transport of aerosols is pronounced in North America (Fischer et al., 2009 and references therein). Overall, it is estimated that sources from eastern Asia contributed 47% of the Pb in the ambient $PM_{2.5}$, local AOSR sources contributed 27%, and regional sources contributed 26% based on the results from the Pb isotope ratio mixing model when merged with the Pb concentration weighted source contributions at Fort McKay over the 2010–2011 sampling period (Table 1).To test the sensitivity of eastern Asian Pb contributions to choice of endmember values, we repeated the calculations using the city from China with the highest and lowest $^{208}Pb/^{207}Pb$ and $^{206}Pb/^{207}Pb$ values rather than the average value from the cities in China (Fig. 3d). The eastern Asia contribution was found to range from 44 to 50%, resulting in a confidence interval for the eastern Asia contribution of 47 ± 3%. The predominant source of Pb emissions from eastern Asia are now fossil fuel (coal) combustion versus leaded gasoline during the 1990s when the PM from the Bollhöfer and Rosman datasets were collected (Li et al., 2012). However, the thorogenic ^{208}Pb signature

Table 1
Pb isotope mixing model Pb source attribution summary.

	% contribution
$PM_{2.5}$ source	
Global (eastern Asia)	47.1
Local (AOSR)	27.0
Regional (western Canada)	25.9
$PM_{10-2.5}$ source	
AOSR Oil Sand	49.7
AOSR Tailings	38.7
AOSR Haul Roads	11.6
Lichen source	
Regional (western Canada)	45.6
Local (AOSR)	31.8
Global (eastern Asia)	22.6

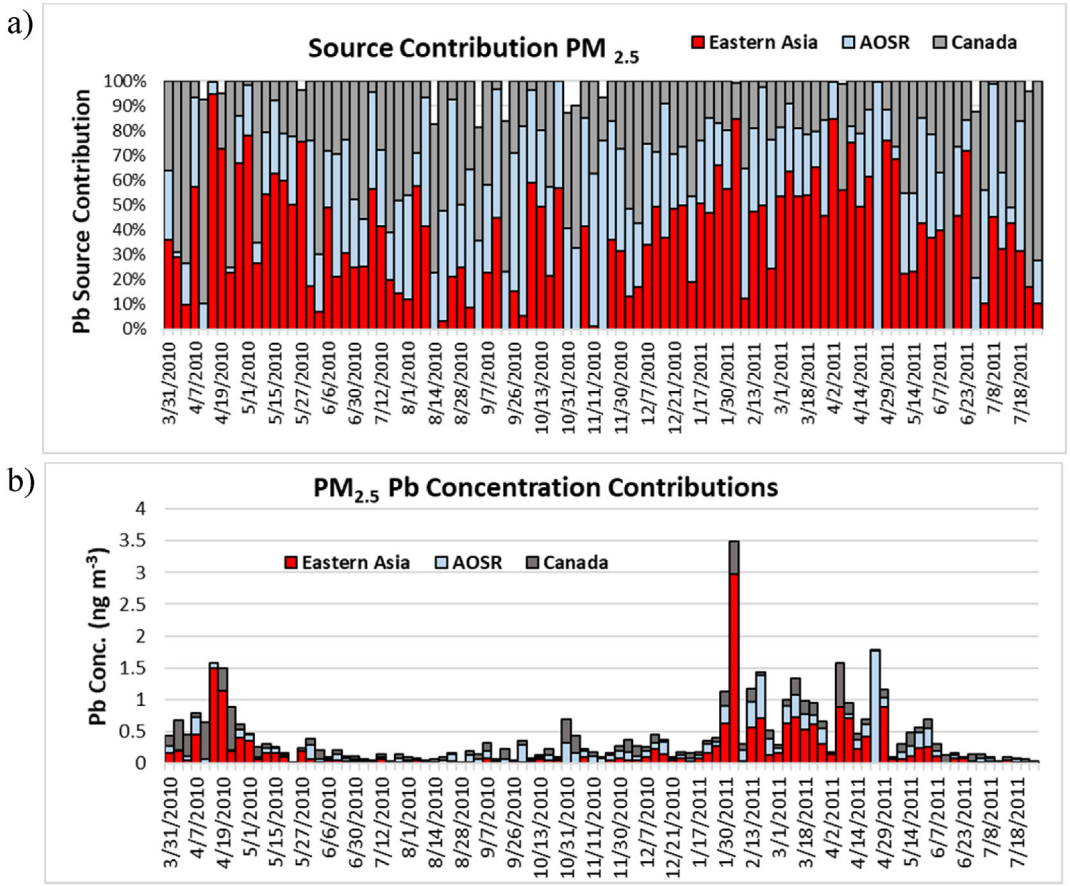

Fig. 5. Temporal Fort McKay $PM_{2.5}$ a) Pb percentage and b) Pb concentration contributions from local (AOSR), regional (Canada) and global (eastern Asia) sources based on the three component Pb isotope ratio mixing model.

is present in coal from China (Tan et al., 2006; Chen et al., 2008) as well as in more recent PM collected in eastern Asia (Chen et al., 2008; Lee et al., 2013; Lee and Yu, 2016). So, although the Pb source contributions from eastern Asia have changed from the 1990s to present, the Pb isotope signature has remained constant.

3.7. Quantifying Pb source contributions in $PM_{10-2.5}$ aerosol samples using Pb isotope ratios

The $^{208}Pb/^{207}Pb$ versus $^{206}Pb/^{207}Pb$ plot of the ambient Fort McKay $PM_{10-2.5}$ also results in a triangular area that encompasses most of the isotope ratio measurements (Fig. 6). PMF results from Landis et al. (2017) indicated the three main contributors to $PM_{10-2.5}$ mass (and the three factors containing the most Pb) were fugitive dust from haul roads, oil sand, and mixed sources. Based on the Pb isotope results from the AOSR source samples (Fig. 3b) and the PMF results, the three endmembers (corresponding to the apices of the triangular field in Fig. 6) include an isotope composition similar to fugitive dust from weathered and fresh oil sand, an endmember with an isotopic composition similar to tailings, and a third endmember that may be a haul road signature (which includes a major contribution from limestone). If we assume that the oil sand, haul roads, and tailings are the three endmembers that comprise the main sources of Pb in the $PM_{10-2.5}$ collected in the AOSR, a three-component mixing model using the values at the apices of the triangle can once again be used to determine the fractional contribution from the three sources on a sample by sample basis. The isotopic compositions used as the model input parameters are found in Table A.1, and the results from this source attribution are presented on a temporal basis in Fig. 7a–b and summarized in Table 1. The temporal results from the $PM_{10-2.5}$ sources do not indicate major differences in fugitive dust source contributions on a seasonal basis (Fig. 7a). The Pb concentration weighted source contributions are lowest between December 2010 and March 2011 when the ground is frozen and snow covers much of the mining operations. Overall based on the results from the Pb isotope ratio mixing model merged with the Pb concentration weighted source contributions (Table 1) at Ft. McKay over the 2010–2011 sampling timeframe, it is estimated that fugitive dust from oil sand contributes 50% of the Pb in the $PM_{10-2.5}$, tailings contributes 39%, while haul roads contribute 12%.

The combined results from the $PM_{10-2.5}$ and $PM_{2.5}$ Pb concentration weighted source attribution (Table 2) indicate contributions of $PM_{2.5}$ from eastern Asia (34%) exceed those from local sources of $PM_{2.5}$ from the AOSR (20%), regional sources of $PM_{2.5}$ (19%), and $PM_{10-2.5}$ fugitive dust from oil sands (14%), tailings (10%), and haul roads (3%).

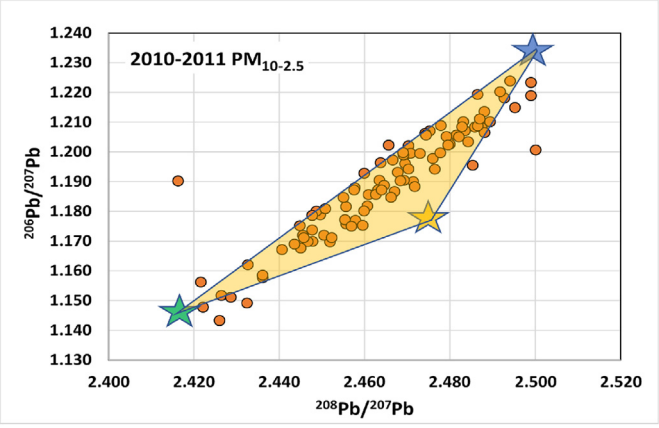

Fig. 6. Fort McKay $PM_{10-2.5}$ Pb isotope results with proposed endmember compositions from AOSR fugitive dust emission sources including oil sand (blue star, upper right), haul roads (brown star, middle right), and tailings (green star, lower left). The triangle encloses most of the Pb isotope ratios from the samples within a three-endmember spatial field.

3.8. Quantifying Pb source contributions in lichen samples from the AOSR using Pb isotope ratios

H. physodes is known to accumulate both $PM_{10-2.5}$ and $PM_{2.5}$ in the AOSR (Graney et al., 2017). Determining the age of *H. physodes* is difficult and we assumed that the samples collected in 2011 integrated and retained a longer term Pb isotope signal than the 16 month time frame when the ambient PM was collected at the Fort McKay BGFM site. The samples from 2008 and 2014 were included to capture longer term variability in Pb source contributions. The $^{208}Pb/^{207}Pb$ versus $^{206}Pb/^{207}Pb$ plot from the lichen samples results in a triangular area that encompasses most of the isotope ratio measurements (Fig. 8). The three apices of the triangle (Fig. 8) likely represent (i) $PM_{10-2.5}$ and $PM_{2.5}$ from the AOSR (local sources), (ii) a global source from eastern Asia as previously indicated by the $PM_{2.5}$ results, and (iii) a regional source that likely includes $PM_{2.5}$ transported to the AOSR from cities in western Canada as well as biomass combustion. Combustion of biomass is now recognized as a large contributor to the PM mass measured in Fort McKay (Landis et al., 2017; Landis et al., 2018) and includes contributions from wildland fires, residential home heating, as well as land clearing operations by the oil sand producers in the AOSR. The triangular field for the lichen dataset has a slightly different global endmember apex than the one used for the ambient Fort McKay $PM_{2.5}$ collected over the 2010–2011 period (Table A.1). It is possible that the average Pb isotope values from sources in China vary and do not always correspond to the average of the values from the four cities in China used previously. Alternatively, a contribution of Pb from non-Chinese sources could also lower the $^{208}Pb/^{207}Pb$ and $^{206}Pb/^{207}Pb$ to an appropriate endmember value to obtain an optimal triangular field for the isotope mixing model (resulting in inclusion of as many data points as possible within the triangular field). For example, inclusion of emissions from the surface mining and processing of the ore deposits in eastern Kazakhstan (average $^{208}Pb/^{207}Pb$ and $^{206}Pb/^{207}Pb$ of 2.431 and 1.149, respectively), the major source of Pb ore used in Russia (Mukai et al., 2001a; Mukai et al., 2001b), would shift the eastern Asian source endmember to slightly lower Pb isotope values after mixing with anthropogenic Pb from China. It is known that anthropogenic sources of Pb and other metals are entrained in the aerosol dust from Asian deserts (east of Kazakhstan) that is transported to North America. Based on results from several PM collection studies in South Korea (Lee et al., 2013; Lee et al., 2015; Lee and Yu, 2016) the anthropogenic signature from eastern Asian sources overwhelms the signature from the natural Pb contained in the desert dust sources. So, the global component apex of the triangular field in Fig. 8 likely represents a mixture of Pb from Kazakhstan and desert sources (minor component) entrained with anthropogenic sources from China (major component).

If the three Pb isotope endmember calculations from the ambient Fort McKay PM results are applied in a similar manner to the lichen data, an estimate of the variability in long-term trans-Pacific transport of aerosols to the AOSR can be obtained by comparing results from lichens collected in 2008, 2011, and 2014. If one uses the metric of distance from the surface oil sands operations to plot the Pb isotope source contribution results, the more distal samples contain a greater proportion of Pb from sources in eastern Asia than the proximal samples in all three collection years (Fig. 9a–c). Stated in another way, even though lichens likely accumulate and integrate multi-source signals over several years, a source contribution from eastern Asia is apparent in all three of the years when the lichens were collected.

Over the 2008–2014 timeframe the results from Pb isotope ratio mixing model merged with the source weighted Pb concentrations in the lichens (Table 1) provides an estimate that regional sources contributed 46% of the Pb in the lichens, local sources contributed 32%, and global sources (eastern Asia) contributed 22%. If the mixing model

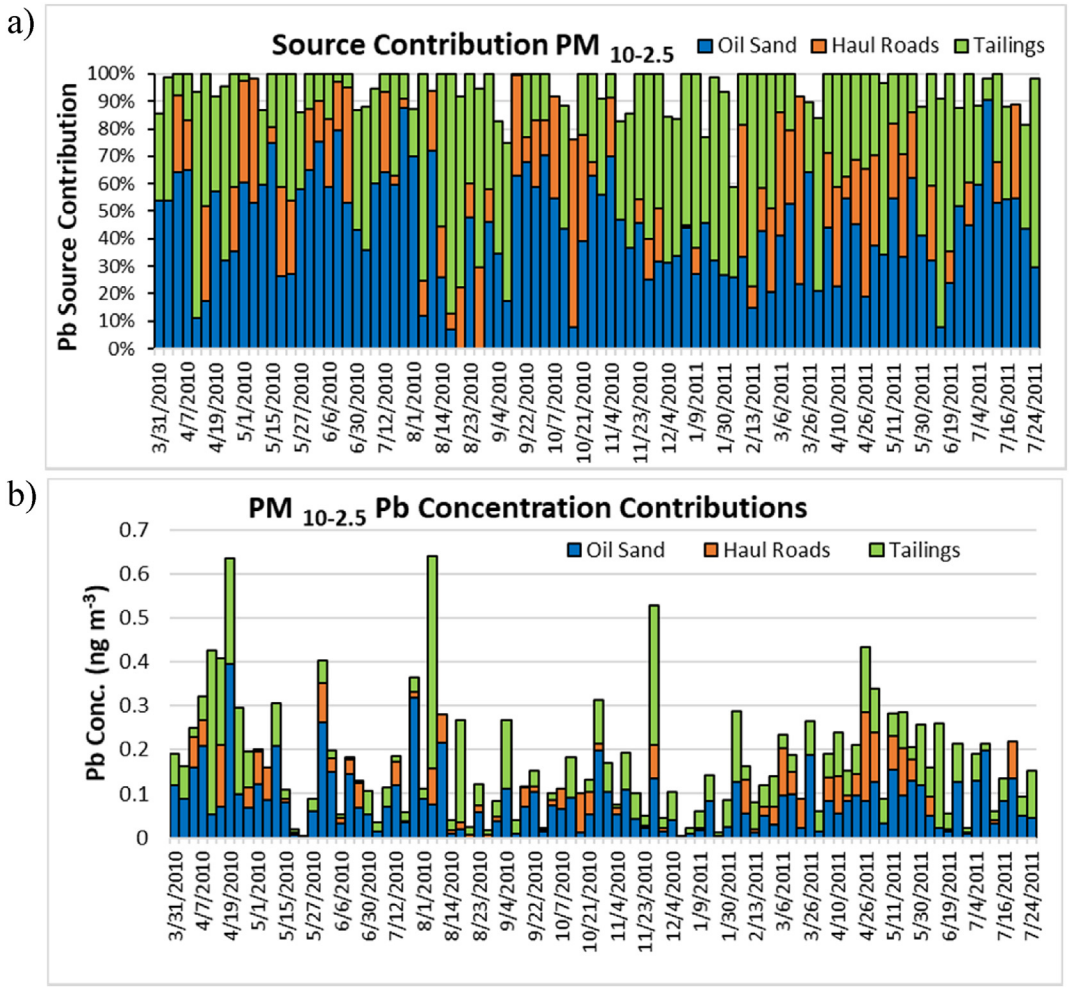

Fig. 7. Temporal Fort McKay $PM_{10-2.5}$ a) Pb percentage and b) Pb concentration contributions from AOSR fugitive emission sources including oil sand, haul roads, and tailings based on the three component Pb isotope ratio mixing model.

results from the proximal lichens (0–30 km) and distal lichens (30–160 km) are separated, local sources predominate at the proximal sites, and regional and global sources are more important at the distal sites (Table 3). The strength of the eastern Asia signal varies from year to year, which is most apparent at the distal lichen locations. The proportion of Pb from eastern Asia at distal sites was greatest in 2011 (41%), with 24% contributions in 2014, and 23% contributions in 2008 (Table 3). This variability likely reflects differing rates of emission from sources as well as differences in PM transport and atmospheric deposition processes at local, regional, and global scales. The contribution of Pb from local fugitive dust sources increased at the proximal sites from 40% in 2008, to 54% in 2011, to 56% in 2014 (Table 3). This increase in fugitive dust contributions corresponds to the expansion of mining and processing activities in the AOSR over the 2008–2014 timeframe (Alberta Energy Regulator, 2018). The greatest proportion of Pb from eastern Asia to the proximal and distal lichens was found in the 2011

Table 2
Combined $PM_{2.5}$ and $PM_{10-2.5}$ Pb source attribution.

2010–2010 PM sources	% contributions
Global $PM_{2.5}$	34.4
Local AOSR $PM_{2.5}$	19.7
Regional $PM_{2.5}$	19.0
AOSR Oil Sand $PM_{10-2.5}$	13.5
AOSR Tailings $PM_{10-2.5}$	10.3
AOSR Haul Roads $PM_{10-2.5}$	3.1

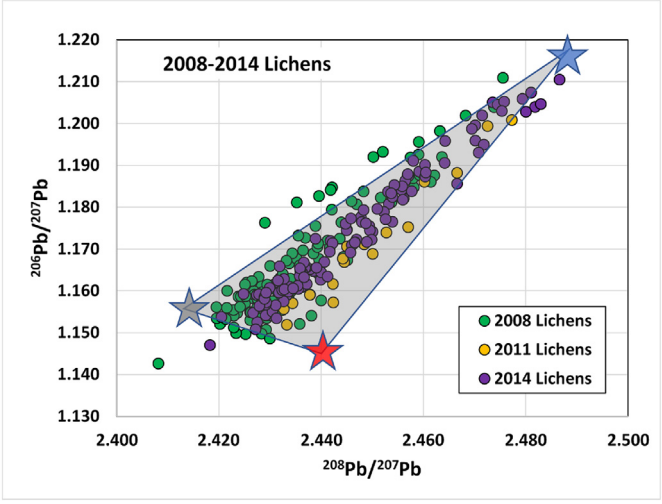

Fig. 8. AOSR lichen Pb isotope results with proposed endmember compositions from local (AOSR $PM_{10-2.5}$ and $PM_{2.5}$ fugitive dust, blue star, upper right), regional (western Canada, gray star, middle left) and global (eastern Asia, red star, lower right) sources. The triangle encloses most of the Pb isotope ratios from the samples within a three-endmember spatial field.

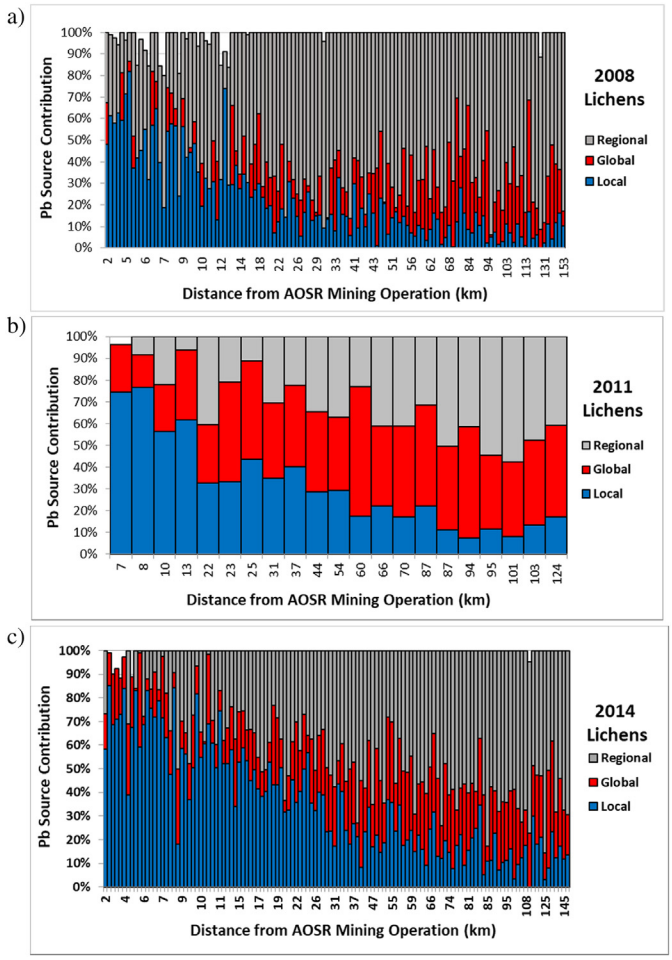

Fig. 9. Percentage of Pb in AOSR lichens from regional (Canada), global (eastern Asia) and local (AOSR) sources based on the three component Pb isotope ratio mixing model portrayed as a function of lichen sampling site distance from the nearest AOSR surface mining operation for a) 2008 lichens (n = 121), b) 2011 lichens (n = 21) and c) 2014 lichens (n = 128).

samples, overlapping with the timeframe when the PM samples were collected for this study.

3.9. Other insights from this study

The Pb isotope signature from materials produced during bitumen upgrading processes is distinct from other sources in the AOSR (Fig. 3b). However, the contribution of emissions from the bitumen upgrading processes in the AOSR in the Fort McKay ambient PM or lichen data sets was difficult to quantify based solely on the Pb isotope ratio findings. The proposed regional Pb isotope signal from western Canada sources likely includes aviation fuel and industrial process as well as coal-fired power plant contributions from far field urban sources. Further work on PM from sites other than Ft. McKay will be needed to better constrain the isotope signatures from these sources. In addition, back trajectory models such as HYSPLIT may offer additional insights concerning global versus regional contributions, after the signatures from local sources of PM have been considered. The contribution from biomass combustion may represent a larger component of the regional signature than anticipated reflecting wildfire, land clearing, and residential heating sources that also needs to be better characterized by further studies. The results from the distal lichen samples (Fig. 3c) likely represent the long term integrated Pb isotope source signature for combusted biomass mixed with far field emissions from urban areas in western Canada, as well as a significant contribution from eastern Asian sources and lesser contributions from stack emissions from the AOSR. Further characterization of source samples from the AOSR, as well as high precision Pb isotope ratio measurements from more sites in western Canada and eastern Asia are needed to refine Pb source contribution estimates in PM in the AOSR.

Table 3
Proximal and distal lichen Pb source attribution percentages.

	2008	2011	2014
Lichen proximal (0–30 km)			
Local	40.4	54.3	56.3
Regional	53.6	16.1	26.9
Global	6.0	29.6	16.8
Lichen distal (30–160 km)			
Local	9.5	18.7	17.0
Regional	67.5	40.9	59.0
Global	23.0	40.8	24.0

4. Conclusions

A novel approach using Pb concentration and isotope ratio measurements and a three-component mixing model was used to quantify local (oil sands mining), regional (western Canada), and global (eastern Asia) atmospheric Pb emission sources within particulate matter (PM) and lichens from the Athabasca Oil Sands Region (AOSR) in northeastern Alberta, Canada. Results from 100 $PM_{2.5}$ and 100 $PM_{10-2.5}$ samples collected over a period of 16 months at the Bertha Ganter Fort McKay monitoring site in 2010–2011 were compared to examine short time interval changes in Pb isotope sources. Results from 250 lichen samples collected in 2008, 2011, and 2014 across a regional scale spatial gradient as far as 160 km from the surface mining operations were compared to include a longer-term temporal component to the study. As far as we are aware this is the largest, most comprehensive dataset that has ever been assembled to compare Pb isotope ratios in PM and lichens on a spatial and temporal basis.

The results from measurements of $^{206}Pb/^{207}Pb$ and $^{208}Pb/^{207}Pb$ isotope ratios from the PM and epiphytic lichens were used to quantify local, regional, and global Pb sources in the PM and lichen data sets using a three-source mixing model. The key for constraining the global source was the recognition of thorogenic ^{208}Pb from eastern Asia sources that plots in a different field in three isotope $^{206}Pb/^{207}Pb$ versus $^{208}Pb/^{207}Pb$ space than the Pb isotope ratios of local source samples from the AOSR.

The Pb isotope ratios associated with many of the $PM_{2.5}$ samples collected in spring 2010 and 2011 were indicative of seasonal trans-Pacific transport of Pb from eastern Asia to the AOSR. Sources from eastern Asia contributed 47 ± 3% of the Pb in the ambient $PM_{2.5}$ in Fort MacKay in 2010–2011. In the combined results from the $PM_{2.5}$ and $PM_{10-2.5}$, contributions of Pb in $PM_{2.5}$ from eastern Asia (34%) exceed local sources of $PM_{2.5}$ Pb from the AOSR (20%), regional sources of $PM_{2.5}$ Pb (19%), and Pb in $PM_{10-2.5}$ from local fugitive dust sources including oil sands (14%), tailings (10%), and haul roads (3%).

Over the 2008–2014 timeframe, regional sources contributed 46% of the Pb in the lichens, local sources contributed 32%, and global sources contributed 22%. If the mixing model results from the near field lichens (0–30 km from surface mining operations) and distal lichens (30–160 km) are separated, local sources of Pb predominate at the near field sites, and regional Pb sources are more prevalent at the distal sites.

A key implication from this study was the ability of the Pb isotope apportionment approach to identify and quantify the amount of trans-Pacific transported Pb in PM superimposed over the aerosol footprint of the world's largest concentration of bitumen mining and upgrading facilities. 47 ± 3% of the Pb within the $PM_{2.5}$ came from eastern Asian sources, which equates to 4.2% of the $PM_{2.5}$ mass in the AOSR from

long distance trans-Pacific transport of Pb. It is remarkable that Pb isotopes could identify this small $PM_{2.5}$ mass contribution in the center of the mining operations in the AOSR. This result demonstrates the sensitivity and utility in using Pb isotope ratios in tracing atmospheric Pb transport processes in future studies within areas with significant local and regional PM sources.

Acknowledgements

This work was funded by the Wood Buffalo Environmental Association (WBEA). The content and opinions expressed by the authors do not necessarily reflect the views of the WBEA or of the WBEA membership. We thank Sanjay Prasad and Gary Cross (WBEA) for managing the ambient sample collection activities in the AOSR; Zack Eastman, Hayley Drake, and Kendra Thomas (WBEA) for ambient sample support; Brad Edgerton (ARA) for filter weighing and logistics, Mike Fort (ARA) for lichen and dichotomous sampler filter extraction and DRC-ICPMS analysis; Keith Puckett for the oversight of the collection of the lichens in 2011 and 2014; and Emily White for improving the quality of the figures. We thank Yu Mei Hsu, Keith Puckett, David Spink, William Studabaker and Emily White for their insights and constructive reviews of the earlier versions of this manuscript. This manuscript is dedicated in memory of Keith Puckett. Keith was a lichenology mentor for the authors, and his professionalism and scientific integrity will not be forgotten.

Appendix A. Supplementary data

Supplementary data to this article can be found online at https://doi.org/10.1016/j.scitotenv.2018.11.047.

References

Alberta Energy Regulator, 2018. https://www.aer.ca Last accessed June 20th, 2018.
Bellis, J.D., Satake, K., Inagaki, M., Zeng, J., Oizumi, T., 2005. Seasonal and long-term change in lead deposition in central Japan: evidence for atmospheric transport from continental Asia. Sci. Total Environ. 341, 149–158.
Bollhöfer, A., Rosman, K.J.R., 2001. Isotopic signatures for atmospheric lead: the Northern Hemisphere. Geochim. Cosmochim. Acta 65, 1727–1740.
Bollhöfer, A., Rosman, K.J.R., 2002. The temporal stability in lead isotopic signatures at selected sites in the Southern and Northern Hemispheres. Geochim. Cosmochim. Acta 66, 1375–1386.
Bory, A.J.M., Abouchami, W., Galer, S.J.G., Svensson, A., Christensen, J.N., Biscaye, P.E., 2014. A Chinese imprint in insoluble pollutants recently deposited in central Greenland as indicated by lead isotopes. Environ. Sci. Technol. 48, 1451–1457.
Carignan, J., Gariepy, C., 1995. Isotopic composition of epiphytic lichens as a tracer of the sources of atmospheric lead emissions in southern Quebec, Canada. Geochim. Cosmochim. Acta 59, 4427–4433.
Carignan, J., Simonetti, A., Gariepy, C., 2002. Dispersal of atmospheric lead in northeastern North America as recorded by epiphytic lichens. Atmos. Environ. 36, 3759–3766.
Chen, J., Tan, M., Li, Y., Zhang, Y., Lu, W., Tong, Y., Zhang, G., Li, Y., 2005. A lead isotope record of Shanghai atmospheric lead emissions in total suspended particles during the period of phasing out of leaded gasoline. Atmos. Environ. 39, 1245–1253.
Chen, J., Tan, M., Li, Y., Zheng, J., Zhang, Y., Shan, Z., Zhang, G., Li, Y., 2008. Characteristics of trace elements and lead isotope ratios in $PM_{2.5}$ from four sites in Shanghai. J. Hazard. Mater. 156, 36–43.
Cheng, H., Hu, Y., 2010. Lead (Pb) isotopic fingerprinting and its applications in lead pollution studies in China: a review. Environ. Pollut. 158, 1134–1146.
Cloquet, C., Carignan, J., Libourel, G., 2006. Atmospheric pollutant dispersal around an urban area using trace metal concentrations and Pb isotopic compositions in epiphytic lichens. Atmos. Environ. 40, 574–587.
Edgerton, E.S., Fort, J.M., Baumann, K., Graney, J.R., Landis, M.S., Berryman, S., Krupa, S., 2012. Method for extraction and multi-element analysis of *Hypogymnia physodes* samples from the Athabasca Oil Sands Region. In: Percy, Kevin (Ed.), Alberta Oil Sands: Energy, Industry and the Environment. Elsevier, Oxford, England, pp. 315–342.
Environment Canada, 2015. Air Pollutant Emission Inventory Report. https://www.canada.ca/en/environment-climate-change/services/air-pollution/publications/emission-inventory-report.html Last accessed February 20th, 2018.
Ewing, S.A., Christensen, J.N., Brown, S.T., Vancuren, R.A., Cliff, S.S., Depaolo, D.J., 2010. Pb isotopes as an indicator of the Asian contribution to particulate air pollution in urban California. Environ. Sci. Technol. 44, 8911–8916.
Faure, G., 1986. Principles of isotope geology. John Wiley & Sons, New York.
Fischer, E.V., Hsu, N.C., Jaffe, D.A., Jeong, M.-J., Gong, S.L., 2009. A decade of dust: Asian dust and springtime aerosol load in the U.S. Pacific Northwest. Geophys. Res. Lett. 36 (L03821).
Gallon, C., Ranville, M.A., Conaway, C.H., Landing, W.M., Buck, C.S., Morton, P.L., Flegal, A.R., 2011. Asian industrial lead inputs to the north Pacific evidenced by lead concentrations and isotopic compositions in surface waters and aerosols. Environ. Sci. Technol. 45, 9874–9882.
Gobeil, C., Johnson, W.K., MacDonald, R.W., Wong, C.S., 1995. Sources and burden of lead in St. Lawrence Estuary sediments: isotopic evidence. Environ. Sci. Technol. 29, 193–201.
Graney, J.R., Landis, M.S., 2013. Coupling meteorology, metal concentrations and Pb isotopes for source attribution in archived precipitation samples. Sci. Total Environ. 448, 141–150.
Graney, J.R., Halliday, A.N., Keeler, G.J., Nriagu, J.O., Robbins, J.A., Norton, S.A., 1995. Isotopic record of lead pollution in lake sediments from the northeastern United States. Geochim. Cosmochim. Acta. 59, 1715–1728.
Graney, J.R., Landis, M.S., Krupa, S., 2012. Coupling lead isotopes and element concentrations in epiphytic lichens to track sources of air emissions in the Athabasca Oil Sands Region. In: Percy, Kevin (Ed.), Alberta Oil Sands: Energy, Industry and the Environment. Elsevier, Oxford, England, pp. 343–372.
Graney, J.R., Landis, M.S., Puckett, K.J., Studabaker, W., Edgerton, E.S., Legge, A., Percy, K.E., 2017. Differential accumulation of PAHs, elements, and Pb isotopes by five lichen species from the Athabasca oil sands region in Alberta, Canada. Chemosphere 184, 700–710.
Gross, B.H., Kreutz, K.J., Osterberg, E.C., McConnell, J.R., Handley, M., Wake, C.P., Yalcin, K., 2012. Constraining recent lead pollution sources in the North Pacific using ice core stable lead isotopes. J. Geophys. Res. 117 (D16307).
Hosono, T., Alvarez, K., Kuwae, M., 2016. Lead isotope ratios in six lake sediment cores from Japan Archipelago: historical record of trans-boundary pollution sources. Sci. Total Environ. 559, 24–37.
Jaffe, D., Anderson, T., Covert, D., Kotchenruther, R., Trost, B., Danielson, J., Simpson, W., Berntsen, T., Karlsdottir, S., Blake, D., Harris, J., Carmichael, G., Itsushi, U., 1999. Transport of Asian air pollution to North America. Geophys. Res. Lett. 26, 711–714.
Jalkanen, L.M., Häsänen, E.K., 1996. Simple method for the dissolution of atmospheric aerosol samples for analysis by Inductively Coupled Plasma Mass Spectrometry. J. Anal. Atomic Spectrom. 11, 365–369.
Kang, J.-H., Hwang, H., Han, C., Hur, S.D., Kim, S.-J., Hong, S., 2017. Pb concentrations and isotopic record preserved in northwest Greenland snow. Chemosphere 187, 294–301.
Komarek, M., Ettler, V., Chrastny, V., Mihaljevic, M., 2008. Lead isotopes in environmental sciences: a review. Environment International 34, 562–577.
Kong, S., Ji, Y., Lu, B., Chen, L., Han, B., Li, Z., Bai, Z., 2011. Characterization of PM_{10} source profiles for fugitive dust in Fushun – a city famous for coal. Atmos. Environ. 45, 5351–5365.
Krachler, M., Le Roux, G., Kober, B., Shotyk, W., 2004. Optimising accuracy and precision of lead isotope measurement (^{206}Pb, ^{207}Pb, ^{208}Pb) in acid digests of peat with ICP-SMS using individual mass discrimination correction. J. Anal. Atomic Spectrom. 19, 354–361.
Landis, M.S., Pancras, J.P., Graney, J.R., Stevens, R.K., Percy, K.E., Krupa, S., 2012. Receptor modeling of epiphytic lichens to elucidate the sources and spatial distribution of inorganic air pollution in the Athabasca Oil Sands Region. In: Percy, Kevin (Ed.), Alberta Oil Sands: Energy, Industry and the Environment. Elsevier, Oxford, England, pp. 427–467.
Landis, M.S., Pancras, J.P., Graney, J.R., White, E., Legge, A., Percy, K.E., 2017. Source apportionment of ambient fine and coarse particulate matter in Fort McKay, Alberta, Canada. Sci. Tot. Environ. 584–585, 105–117.
Landis, M.S., Kamal, A.S., Edgerton, E.S., Wentworth, G., Sullivan, A.P., Dillner, A.M., 2018. The impact of the 2016 Fort McMurray Horse River Wildfire on ambient air pollution levels in the Athabasca Oil Sands Region, Alberta, Canada. Sci. Tot. Environ. 618, 1665–1676.
Lee, P.K., Yu, S., 2016. Lead isotopes combined with a sequential extraction procedure for source apportionment in the dry deposition of Asian dust and non-Asian dust. Environ. Pollut. 210, 65–75.
Lee, P.-K., Youm, S.-J., Jo, H.Y., 2013. Heavy metal concentrations and contamination levels from Asian dust and identification of sources: a case-study. Chemosphere 91, 1018–1025.
Lee, P.K., Jo, H.Y., Kang, M.J., Kim, S.O., 2015. Seasonal variation in trace element concentrations and Pb isotopic composition of airborne particulates during Asian dust and non-Asian dust periods in Daejeon, Korea. Environ. Earth Sci. 74, 3613–3628.
Li, Q., Cheng, H., Zhou, T., Lin, C., Guo, S., 2012. The estimated atmospheric lead emissions in China. Atmos. Environ. 60, 1–8.
Loo, B.W., Cork, C.P., 1998. Development of high efficiency virtual impactors. Aerosol Sci. Technol. 9, 167–176.
McFarland, A.R., Ortiz, C.A., Bertch Jr., R.W., 1978. Particle collection characteristics of a single stage dichotomous sampler. Environ. Sci. Technol. 12, 679–682.
Mukai, H., Furuta, N., Fujii, T., Ambe, Y., Sakamoto, K., Hashimoto, Y., 1993. Characterizations of sources of lead in the urban air of Asia using ratios of stable lead isotopes. Environ. Sci. Technol. 27, 1347–1356.
Mukai, H., Tanaka, A., Fujii, T., Zeng, Y., Hong, Y., 2001a. Regional characteristics of sulfur and lead isotope ratios at several Chinese urban sites. Environ. Sci. Technol. 35, 1064–1071.
Mukai, H., Machida, T., Tanaka, A., Pavel Vera, Y., Uematsu, M., 2001b. Lead isotope ratios in the urban air of eastern and central Russia. Atmos. Environ. 35, 2783–2793.
Osterberg, E.C., Mayewski, P., Kreutz, K., Fisher, D., Handley, M., Sneed, S., Zdanowicz, C., Zheng, J., Demuth, M., Waskiewicz, M., Bourgeois, J., 2008. Ice core record of rising lead pollution in the North Pacific atmosphere. Geophys. Res. Lett. 35 (L05810) (427 doi:05810.01029/02007GL032680).
Pancras, J.P., Vedantham, R., Landis, M.S., Norris, G.A., Ondov, J.M., 2011. Application of EPA Unmix and nonparametric wind regression on high time resolution trace

elements and speciated mercury in Tampa, Florida aerosol. Environ. Sci. Technol. 45, 3511–3518.
Schleicher, N., Norra, S., Chai, F., Chen, Y., Wang, S., Cen, K., Yu, Y., Stüben, D., 2011. Temporal variability of trace metal mobility of urban particulate matter from Beijing-a contribution to health impact assessments of aerosols. Atmos. Environ. 45, 7248–7265.
Shotyk, W., Appleby, P.G., Bicalho, B., Davies, L.J., Froese, D., Grant-Weaver, I., Magnan, G., Mullan-Boudreau, G., Noernberg, T., Pelletier, R., Shannon, B., van Bellen, S., Zaccone, C., 2017. Peat bogs document decades of declining atmospheric contamination by trace metals in the Athabasca Bituminous Sands region. Environ. Sci. Technol. 51, 6237–6249.
Simonetti, A., Gariépy, C., Carignan, J., 2003. Tracing sources of atmospheric pollution in western Canada using Pb isotopic composition and heavy metal abundances in epiphytic lichens. Atmos. Environ. 37, 2853–2865.
Tan, M.G., Zhang, G.L., Li, X.L., Zhang, Y.X., Yue, W.S., Chen, J.M., Wang, Y.S., Li, A.G., Li, Y., Zhang, Y.M., Shan, Z.C., 2006. Comprehensive study of lead pollution in Shanghai by multiple techniques. Anal. Chem. 78, 8044–8050.
U.S. Environmental Protection Agency, March 2015. The 2011 National Emissions Inventory, Version 2. Office of Air Quality Planning and Standards, Research Triangle Park, NC, USA https://www.epa.gov/air-emissions-inventories/2011-national-emissions-inventory-nei-data Last accessed March 1, 2018.
Uematsu, M., Duce, R.A., Prospero, J.M., Chen, L., Merrill, J.T., McDonald, R.L., 1983. Transport of mineral aerosol from Asia over the North Pacific Ocean. J. Geophys. Res. 88, 5343–5352.
VanCuren, R.A., 2003. Asian aerosols in North America: extracting the chemical composition and mass concentration of the Asian continental aerosol plume from long-term aerosol records in the western United States. J. Geophys. Res. Atmos. 108, 4263.
VanCuren, R.A., Cahill, T.A., 2002. Asian aerosols in North America: frequency and concentration of fine dust. J. Geophys. Res. 107, 4804.
Wang, W., Liu, X., Zhao, L., Guo, D., Tian, X., Adams, F., 2006. Effectiveness of leaded petrol phase-out in Tianjin, China based on the aerosol lead concentration and isotope abundance ratio. Sci. Total Environ. 364, 175–187.
Wang, X., Watson, J.G., Chow, J.C., Kohl, S.D., Chen, L.-W.A., Sodeman, D.A., Legge, A.H., Percy, K.E., 2012. Measurement of real-world stack emissions with a dilution sampling system. In: Percy, Kevin (Ed.), Alberta Oil Sands: Energy, Industry and the Environment. Elsevier, Oxford, England, pp. 171-–192.
Wang, P., Cao, J., Shen, Z., Han, Y., Lee, S., Huang, Y., Zhu, C., Wang, H., Huang, R., 2015a. Spatial and seasonal variations of $PM_{2.5}$ mass and species during 2010 in Xian China. Sci. Total Environ. 508, 477–487.
Wang, X., Chow, J.C., Kohl, S.D., Percy, K.E., Legge, A.H., Watson, J.G., 2015b. Characterization of $PM_{2.5}$ and PM_{10} fugitive dust source profiles in the Athabasca Oil Sands Region. J. Air Waste Manag. 65, 1421–1433.
Wang, X., Chow, J.C., Kohl, S.D., Percy, K.E., Legge, A.H., Watson, J.G., 2016. Real-world emission factors for Caterpillar 797B heavy haulers during mining operations. Particuology 28, 22–30.
Watson, J.G., Chow, J.C., Wang, X., Kohl, S.D., Chen, L.-W.A., Etyemezian, V., 2012. Overview of real-world emission characterization methods. In: Percy, Kevin (Ed.), Alberta Oil Sands: Energy, Industry and the Environment. Elsevier, Oxford, England, pp. 145–170.
Widory, D., Liu, X., Dong, S., 2010. Isotopes as tracers of sources of lead and strontium in aerosols (TSP & $PM_{2.5}$) in Beijing. Atmos. Environ. 44, 3679–3687.
Yienger, J.J., Galanter, M., Holloway, T.A., Phadnis, M.J., Guttikunda, S.K., Carmichael, G.R., Moxim, W.J., Levy II, H., 2000. The episodic nature of air pollution transport from Asia to North America. J. Geophys. Res. 106, 26931–26,945.
Yip, Y., Chung-wah Lamb, J., Tong, W., 2008. Applications of lead isotope ratio measurements. Trends Anal. Chem. 27, 460–480.
Zdanowicz, C., Hall, G., Vaive, J., Amelin, Y., Percival, J., Girard, I., Biscaye, P., Borys, A., 2006. Asian dustfall in the St. Elias Mountains, Yukon, Canada. Geochim. Cosmochim. Acta 70, 3493–3507.
Zheng, J., Tan, M., Shibata, Y., Tanaka, A., Li, Y., Zhang, G., Zhang, Y., Shan, Z., 2004. Characteristics of lead isotope ratios and elemental concentrations in PM_{10} fraction of airborne particulate matter in Shanghai after the phase-out of leaded gasoline. Atmos. Environ. 38, 1191–1200.
Zhou, S., Davy, P.K., Wang, X., Cohen, J.B., Liang, J., Huang, M., Fan, Q., Chen, W., Chang, M., Ancelet, T., Trompetter, W.J., 2016. High time-resolved elemental components in fine and coarse particles in the Pearl River Delta region of Southern China: dynamic variations and effects of meteorology. Sci. Total Environ. 572, 634–664.